SUPPLEMENTARY INFORMATION

Detecting the Structural Assembly Pathway of Human Antimicrobial Peptide Pores at Single-channel level

Neethu Puthumadathil[1,2], Poornendhu Jayasree[1], K Santhosh Kumar[1], K Madhavan Nampoothiri[3] Harsha Bajaj[3], Kozhinjampara R Mahendran[1]*

[1]Membrane Biology Laboratory, Interdisciplinary Research Program, Rajiv Gandhi Centre for Biotechnology, Thiruvananthapuram 695014, India.

[2]Manipal Academy of Higher Education, Manipal, Karnataka, India-576104

[3]Microbial Processes and Technology Division, CSIR- National Institute for Interdisciplinary Science and Technology (NIIST), Thiruvananthapuram 695019, India

*To whom correspondence should be addressed

*e-mail: mahendran@rgcb.res.in

Supplementary Materials:

The following materials were used for the study: 1,2-diphytanoyl-*sn*-glycero-3-phosphocholine (DPhPC, Avanti Polar Lipids), *E. coli* polar Lipid Extract (Avanti Polar Lipids), pentane (Sigma-Aldrich), hexadecane (Sigma-Aldrich), n-dodecyl β-D-maltoside (DDM, Sigma-Aldrich), sodium dodecyl sulfate (SDS, Sigma-Aldrich), potassium chloride (Sigma-Aldrich), 2-(N-morpholino)ethanesulfonic acid (MES, Sigma-Aldrich), dextran (MW 40,000, Sigma-Aldrich), ethylenediaminetetraacetic acid disodium salt (EDTA, Sigma-Aldrich), sodium chloride (Sigma-Aldrich), 2-Propanol (Sigma-Aldrich), Acetone(Sigma-Aldrich), all other reagent (Sigma-Aldrich). 2x Laemmli sample buffer (Bio-Rad), Any kD™ Mini-PROTEAN® TGX™ precast gel (Bio-Rad), Precision Plus Protein™ Dual Color Standards (Bio-Rad), All dermcidin peptides were *purchased* from Peptide Protein Research Ltd at >95% purity (HPLC) as lyophilized powders.

Supplementary Text:

a) Methods to create the molecular models of dermcidin peptide pores:

The structure of DCD-1L represented in figures is based on the crystal structure of dermcidin[1] (PDB:2YMK). The structure of DCD SSL-25 is modeled based on the crystal structure of dermcidin comprising six peptide monomers arranged in parallel. The APBS electrostatics plugin in PyMOL was exploited to understand the electrostatic charge distribution in the different models for both the peptides.

b) Ion selectivity measurements through DCD peptide pores:

The current recordings were performed by establishing a KCl concentration gradient across the peptide pore. The potential difference was applied through Ag/AgCl electrodes with agarose salt bridges. 1M KCl at the cis side and 150mM of KCl at the trans side were added to the bilayer chamber. Subsequently, the channel insertion resulted in the current at 0 mV. This ionic current was manually set to zero by adjusting the applied voltage. The voltage required to achieve zero current is known as the 'reverse potential' (V_m), which can be used to calculate the permeability ratio of K^+ and Cl^- ions across the pore by Goldman-Hodgkin-Katz equation[2].

$$V_m = \frac{RT}{F} \ln \left(\frac{P_{K^+}[K^+]^{cis} + P_{Cl^-}[Cl^-]^{trans}}{P_{K^+}[K^+]^{trans} + P_{Cl^-}[Cl^-]^{cis}} \right)$$

In this equation *R* is the universal gas constant (8.314 $J.K^{-1}.mol^{-1}$), *T* is the temperature in Kelvin (K = °C + 273.15), *F* is the Faraday's constant (96485 $C.mol^{-1}$), P_K is the membrane permeability for K^+, P_{Cl} is the relative membrane permeability for Cl^-, $[K^+]^{cis}$ is the concentration of K^+ in the cis side, $[K^+]^{trans}$ is the concentration of K^+ in the trans side, $[Cl^-]^{cis}$ is the concentration of Cl^- in the cis side and $[Cl^-]^{trans}$ is the concentration of Cl^- in the trans side. We derived the permeability ratio of K^+ and Cl^- ions P_{K+}/ P_{Cl-} based on this equation.

c) Gel extraction of DCD peptides:

The DCD-1L and SSL-25 peptides were loaded on a Mini-PROTEAN® TGX™ precast gel (Bio-Rad) with Protein Standard Marker (Bio-Rad) followed by SDS PAGE. Bands containing peptide monomers were cut from the gel and each gel slice was solubilized with 10 mM phosphate buffer (K_2HPO_4, pH 7.4, 500 µL) and crushed with a plastic pestle. After 30 min at room temperature, the gel fragments were removed with a microfilterfuge tubes by centrifugation at 15,000 xg. The filtrate contained the peptide monomer was used to test the channel-forming activity in the single-channel electrical recordings.

d) Circular dichroism spectroscopy

Circular dichroism spectra were obtained using Jasco J-810 spectropolarimeter. Peptide samples were prepared as 25 µM solution in phosphate buffered saline (PBS, 8.2 mM sodium phosphate, 1.8 mM potassium phosphate, 137 mM sodium chloride, 2.7 mM potassium chloride at pH 7.4) with 1% DDM or 1% SDS. Spectra were collected using a 1 mm path length quartz cuvette at 20 °C. For each dataset (in deg), baselines from the same buffer and cuvette were subtracted, and then data points were normalized for amide bond concentration and path length to give mean residue ellipticity (MRE; deg cm^2 $dmol^{-1}$ res^{-1}).

e) Liposome permeation assay:

Swelling assays were performed with *E. coli* total lipid extract as described previously with minor modifications[3]. Here, 2 mg of lipid was used to form a lipid film that was dried and dissolved in diethyl ether. A thin film was formed using nitrogen gas and dried overnight or for few hours in desiccator. The film was resuspended in 20 mM phosphate buffer pH 6 (200 µL) (control) or buffer

including 1 µM of peptide and incubated at 30°C for 30 minutes. The resulting solution was sonicated for 45 seconds and a film was made in a water bath at 50 °C using a Rotavapor. The lipid-protein mixture was dried in a desiccator vacuum overnight. The film was resuspended in 20 mM phosphate buffer pH 6 (600 µL) containing 15% dextran (MW 40,000) by slowly adding the latter to the side of the test-tube and gently rotating the tube to wet the film. The tubes were incubated at 37°C for 45 min, shaken by hand and incubated for another 30 min. The concentrations of test solute were adjusted so that diluents were isotonic with control liposomes. Raffinose was also tested with proteoliposomes to confirm the isotonicity of the multilamellar liposomes. Liposome or proteoliposome solution (45 µL) was diluted into 995 µL of an isotonic test/solute solution made in 20 mM phosphate buffer pH 6 buffer in a 1 mL cuvette and mixed manually. The change in absorbance at 500 nm was monitored using a UV-2600 Shimadzu spectrophotometer in the kinetic measurement mode. The swelling rates were calculated as the change in absorbance min^{-1} which reflects swelling of liposomes. The rates are taken as averages from 3 different sets of experiments.

Supplementary Figures:

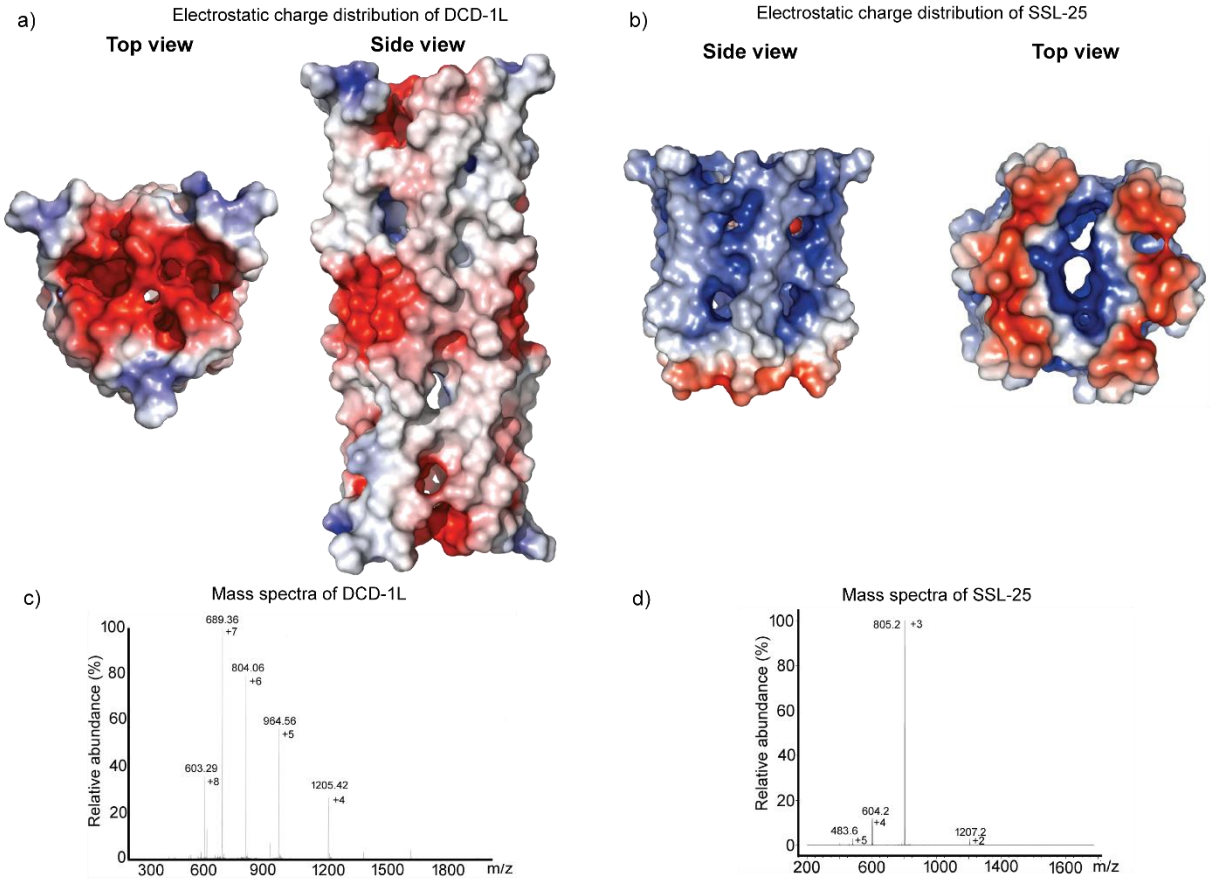

Figure. S1: Modeled DCD channels with electrostatic charge distribution.

a) Structure of the DCD-1L peptide pore. Side view and top view. **b)** Structure of the modeled DCD SSL-25 peptide. Side view and top view. Negatively charged regions are highlighted in red color. Positively charged regions highlighted in blue color and neutral regions in white. **c)** Mass spectrum of DCD -1L peptide Calculated mass = 4818.5 Da, observed mass = 4818.48 Da **d)** Mass spectrum of DCD-SSL25. Calculated mass = 2412.8 Da, observed mass =2412.79 Da.

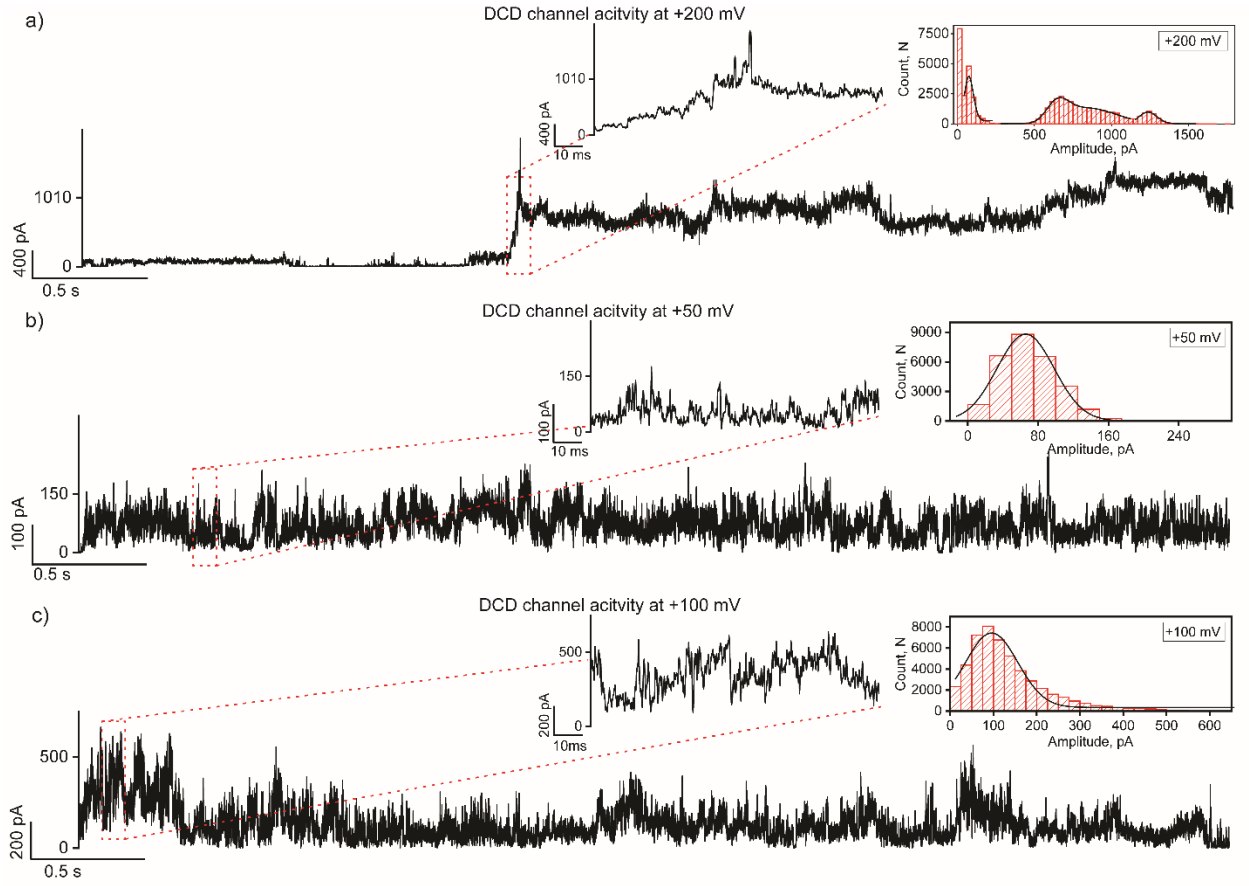

Figure. S2: Electrical recordings of dermcidin in planar lipid bilayers

a) Electrical recording of DCD-1L peptides inserting into the planar lipid bilayers at +200 mV. Electrical recordings of DCD-1L peptide channel showing transient open conductance states that fluctuated into different conductance states and noisy gating events at **b)** +50 mV, **c)** +100 mV. Inset represents corresponding all points current amplitude histogram and ion current recordings at expanded time scale. Reaction conditions: 1M KCl, 10mM MES, pH 6.0, 1mM $ZnCl_2$.

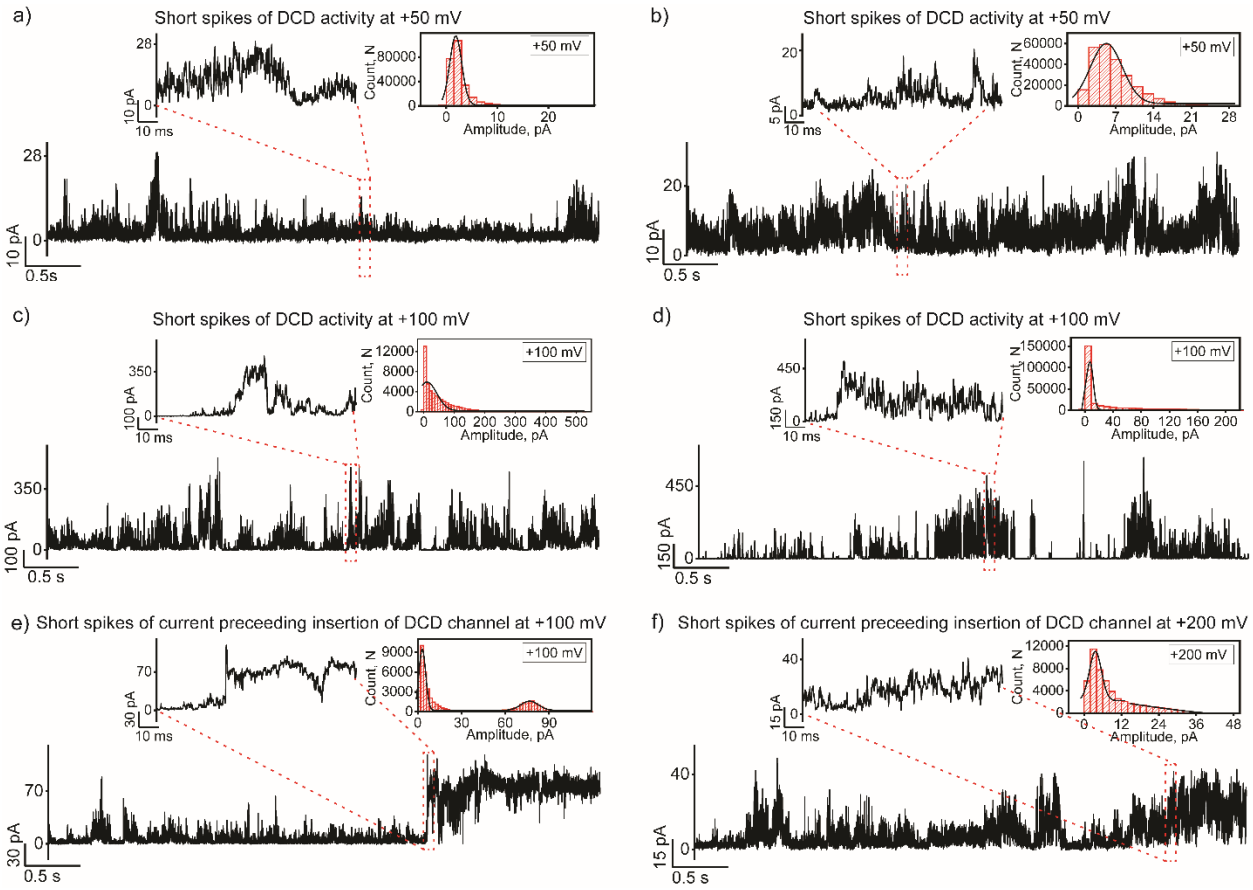

Figure S3: Electrical recordings of dermcidin membrane insertion and channel activity in planar lipid bilayers.

Electrical recording showing the membrane association of DCD-1L peptides into planar lipid bilayers exhibiting short, frequent temporal spikes at different voltages **a)** +50 mV, **b)** +50 mV, **c)** +100 mV, **d)** +100 mV. The membrane insertion of the DCD peptides resulting in the fluctuating channel of diverse conductance states at different voltages **e)** +100 mV, **f)** +200 mV. Inset represents corresponding all points current amplitude histogram and ion current recordings at expanded time scale. Reaction conditions: 1M KCl, 10 mM MES, pH 6.0, 1mM $ZnCl_2$.

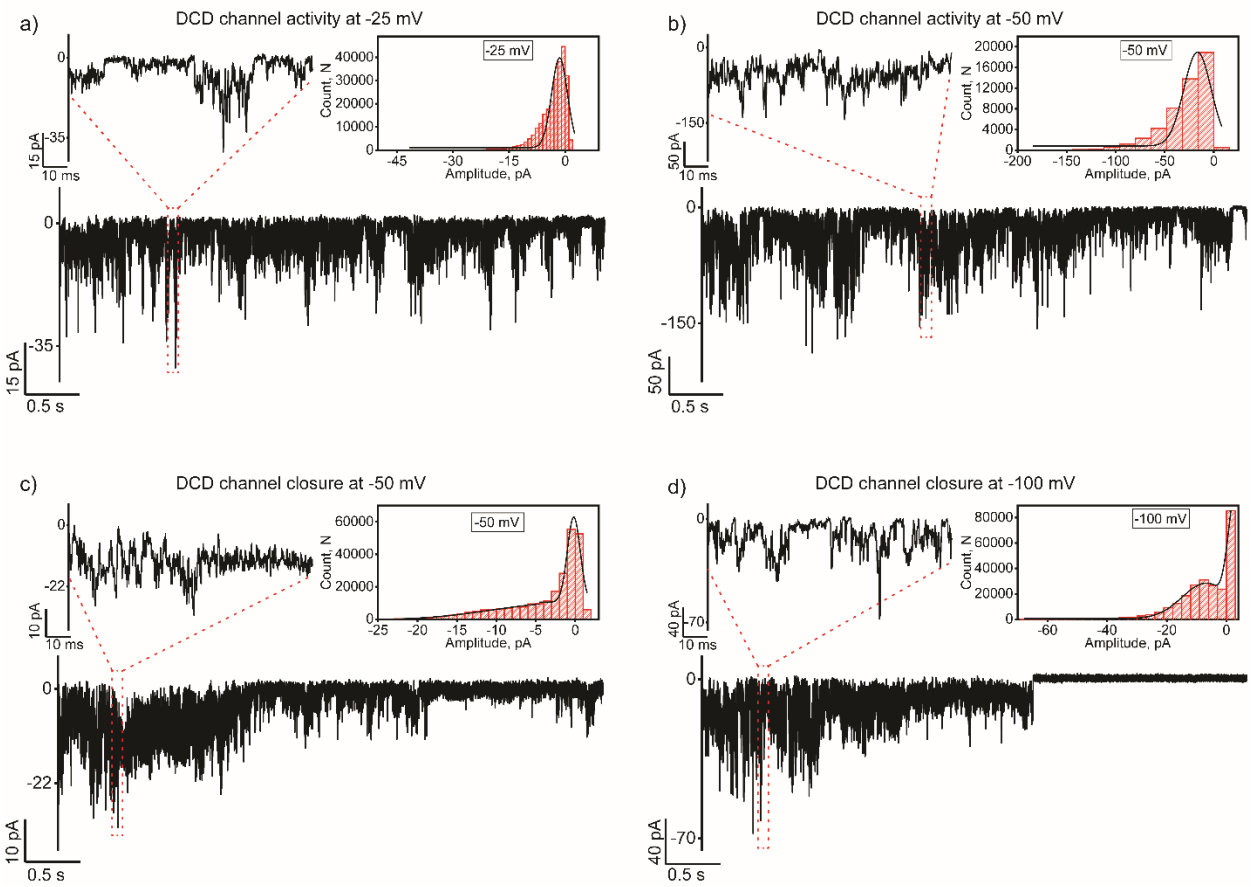

Figure S4: Electrical recordings of dermcidin in planar lipid bilayers at negative voltages

a) Electrical recording of DCD-1L peptide pores in planar lipid bilayer at -25 mV. **b)** Electrical recording of DCD channel showing transient noisy pore openings at -50 mV. **c)** Electrical recording of DCD channel showing increased gating of the channel resulting in complete closure at -50 mV and **d)** -100 mV. Inset represents corresponding all points current amplitude histogram and ion current recordings at expanded time scale. Reaction conditions: 1M KCl, 10mM MES, pH 6.0, 1mM $ZnCl_2$.

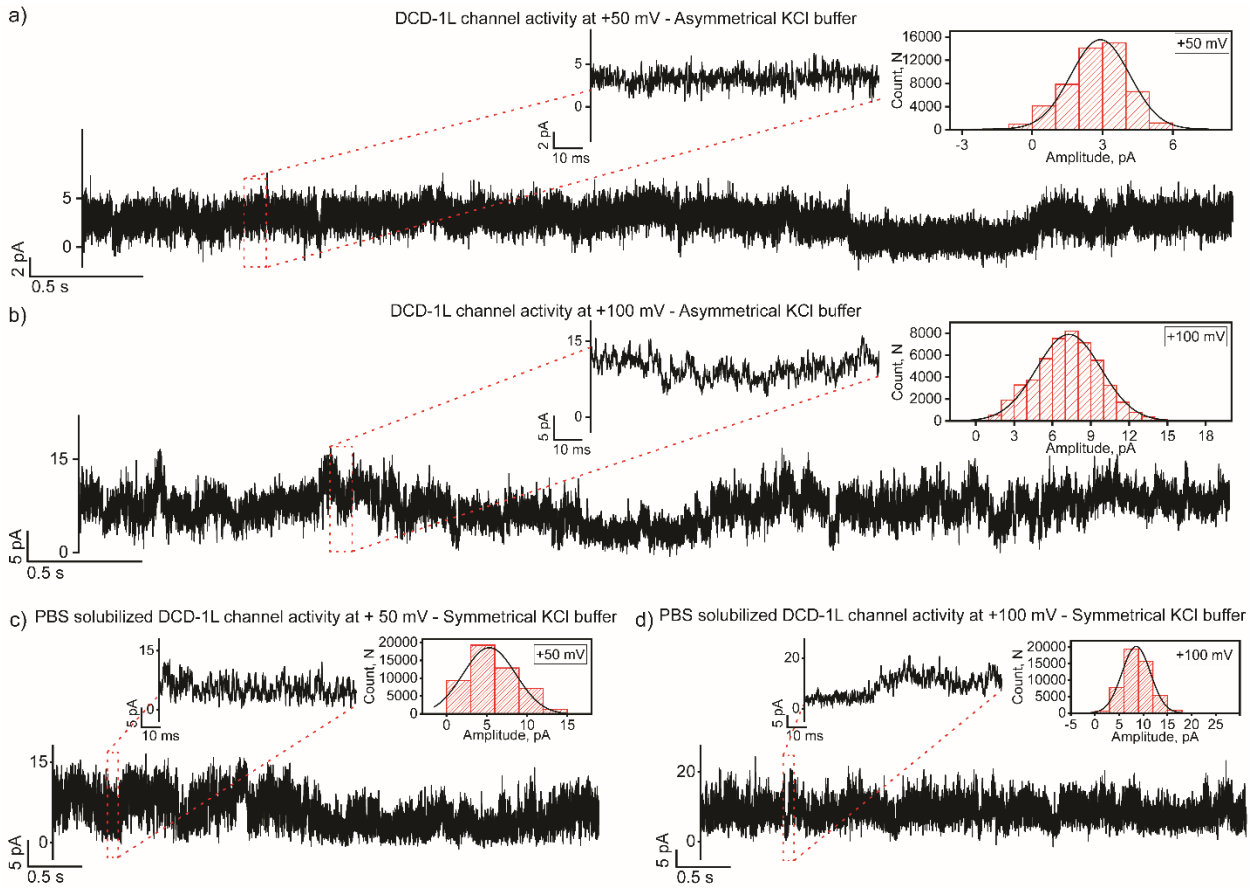

Figure S5: Electrical recording of dermcidin in planar lipid bilayer

a) Electrical recording of the DCD-1L channel at +50 mV showing fluctuating conductance states. **b)** Electrical recording of the DCD-1L channel at +100 mV showing fluctuating noisy conductance states with frequent gating events. Reaction conditions: 1M KCl, 10mM MES, pH 6.0, 1mM $ZnCl_2$ cis/ 0.15 M KCl, 10 mM MES, pH 6.0 trans, 1mM $ZnCl_2$. **c)** Electrical recording of the PBS solubilized DCD-1L channel at +50 mV and +100 mV showing fluctuating noisy conductance states with frequent gating events. Inset represents corresponding all points current amplitude histogram and ion current recordings at expanded time scale. Reaction conditions: 1M KCl, 10mM MES, pH 6.0, 1mM $ZnCl_2$.

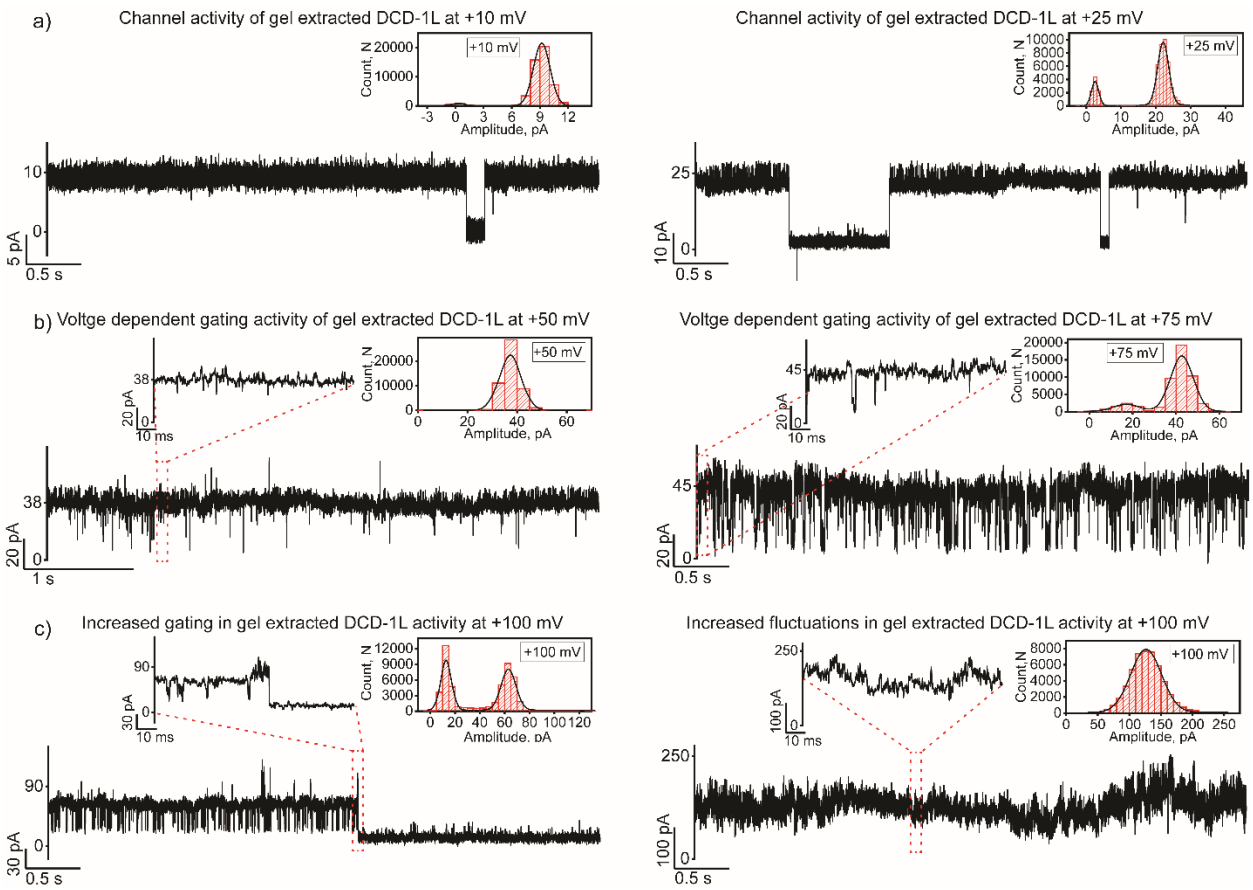

Figure S6: Electrical recordings of gel extracted DCD in planar lipid bilayers

a) Electrical recording of gel extracted DCD-1L peptide reconstituted in planar lipid bilayer showing stable channel at +10 mV and +25 mV. **b)** Electrical recording of gel extracted DCD-1L peptide showing stable channel with gating events at +50 mV and +75 mV. **c)** Electrical recording of gel extracted DCD-1L peptide showing channel with increased noisy gating events with different sub-conductance states at +100 mV. Inset represents corresponding all points current amplitude histogram and ion current recordings at expanded time scale. Reaction conditions: 1M KCl, 10mM MES, pH 6.0, 1mM $ZnCl_2$.

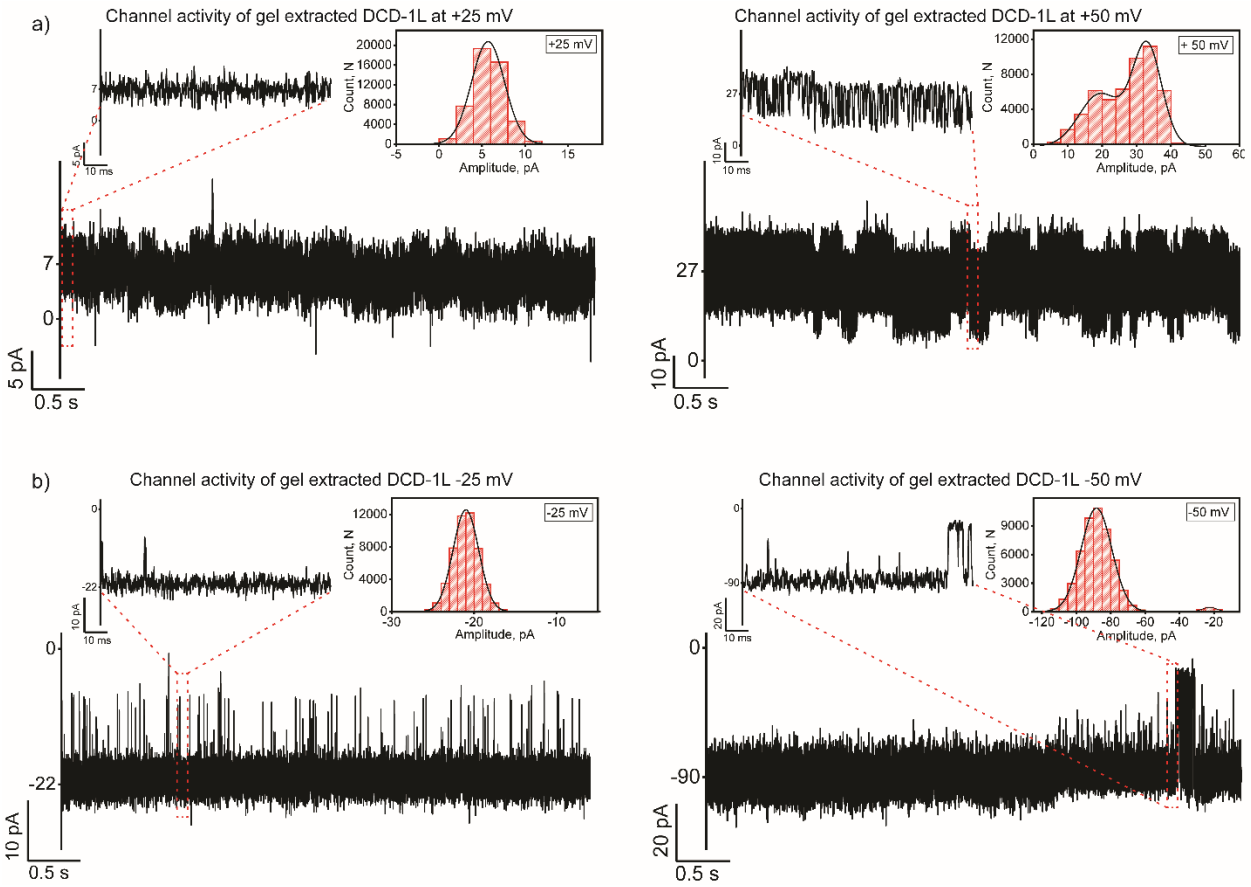

Figure S7: Electrical recordings of gel extracted DCD in planar lipid bilayers in asymmetrical salt conditions

Electrical recording of gel extracted DCD-1L peptide reconstituted in planar lipid bilayer showing a stable channel at **a)** +25 mV and +50 mV **b)** -25 mV and -50 mV. The corresponding all points current amplitude histogram is shown confirming the asymmetry in the ion conductance and channel rectification. Inset shows ion current recordings at expanded time scale. Reaction conditions: 1M KCl, 10mM MES, pH 6.0, 1mM $ZnCl_2$/ 0.15 M KCl, 10 mM MES, pH 6.0, 1mM $ZnCl_2$, trans.

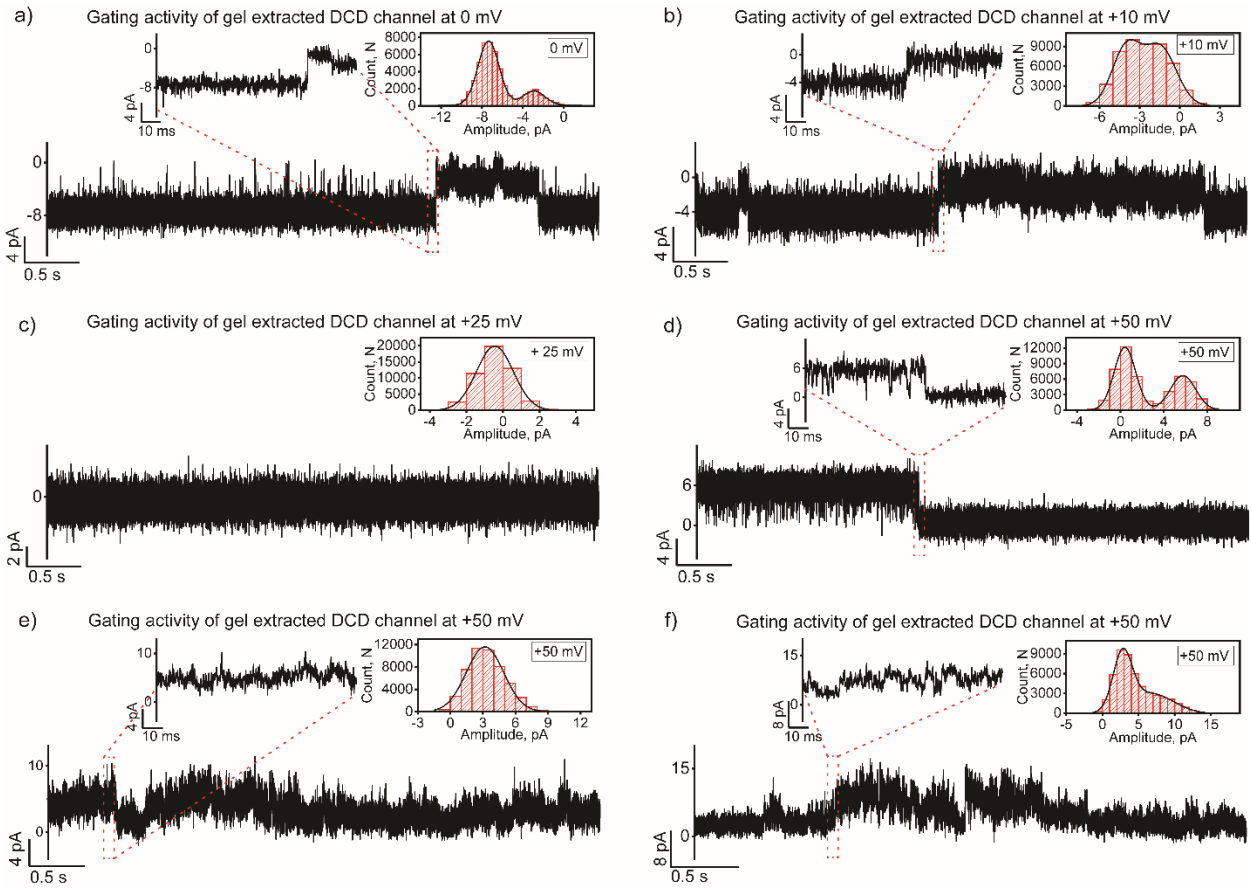

Figure S8: Electrical recordings of gel extracted DCD showing gating in planar lipid bilayers in asymmetrical conditions

Electrical recording of gel extracted DCD-1L peptide reconstituted in planar lipid bilayer showing various gating patterns at different voltages **a)** 0 mV, **b)** +10 mV, **c)** +25 mV and **d)** +50 mV. **e), f)** Electrical recording of gel extracted DCD-1L peptide showing highly gated fluctuating channel at + 50 mV. Inset represents corresponding all points current amplitude histogram and ion current recordings at expanded time scale. Reaction conditions: 1M KCl, 10mM MES, pH 6.0, 1mM $ZnCl_2$, cis/ 0.15 M KCl, 10 mM MES, pH 6.0, 1mM $ZnCl_2$,trans.

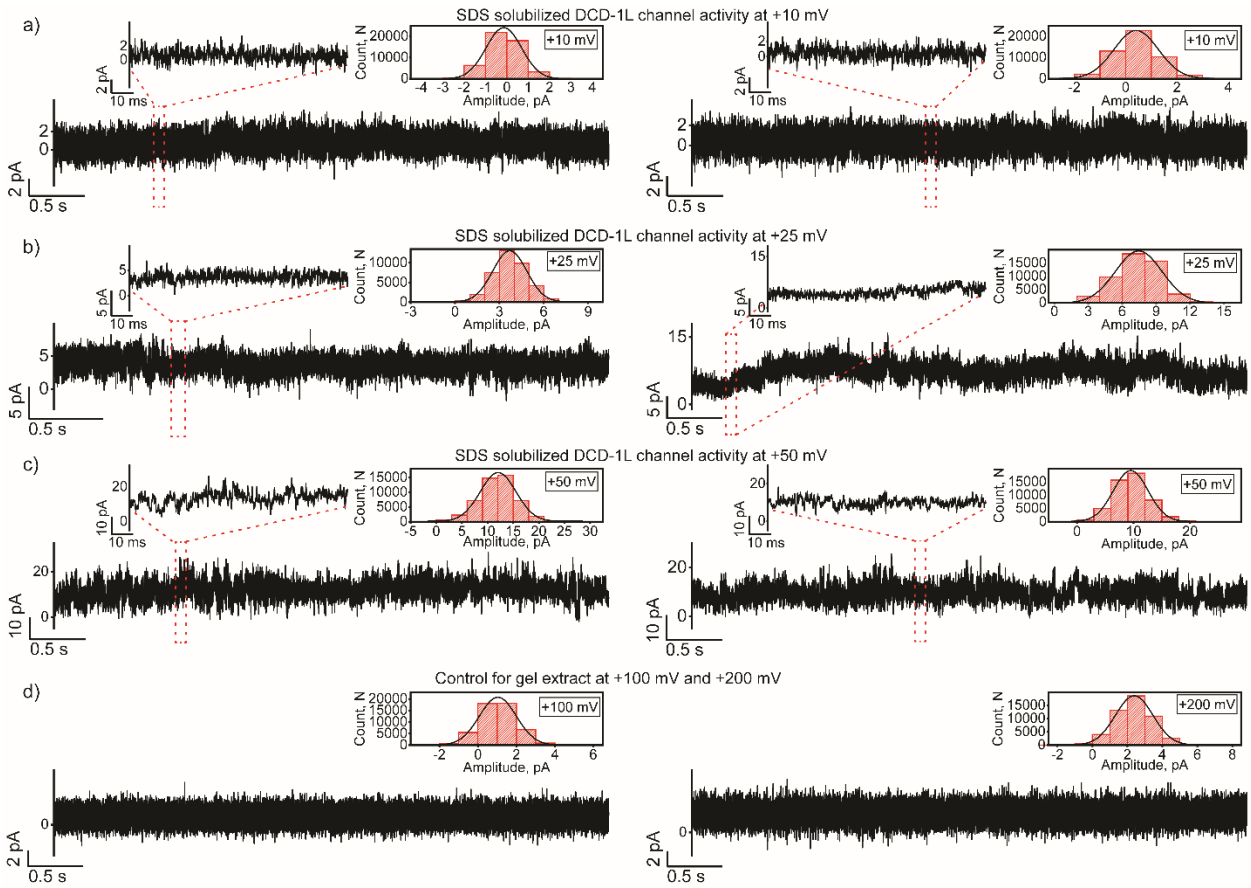

Figure S9: Electrical recordings of SDS-solubilized dermcidin in planar lipid bilayers

a) Electrical recording of SDS solubilized DCD-1L peptide pores in planar lipid bilayer at +10 mV. **b)** Electrical recording of DCD-1Lchannel showing channel activity at +25 mV. **c)** Electrical recording of DCD-1L channel activity with increased gating events at +50 mV. Inset represents corresponding all points current amplitude histogram and ion current recordings at expanded time scale. **d)** Gel extract without DCD peptide band that did not show any channel activity at +100 mV and +200 mV. Reaction conditions: 1M KCl, 10mM MES, pH 6.0, 1mM $ZnCl_2$.

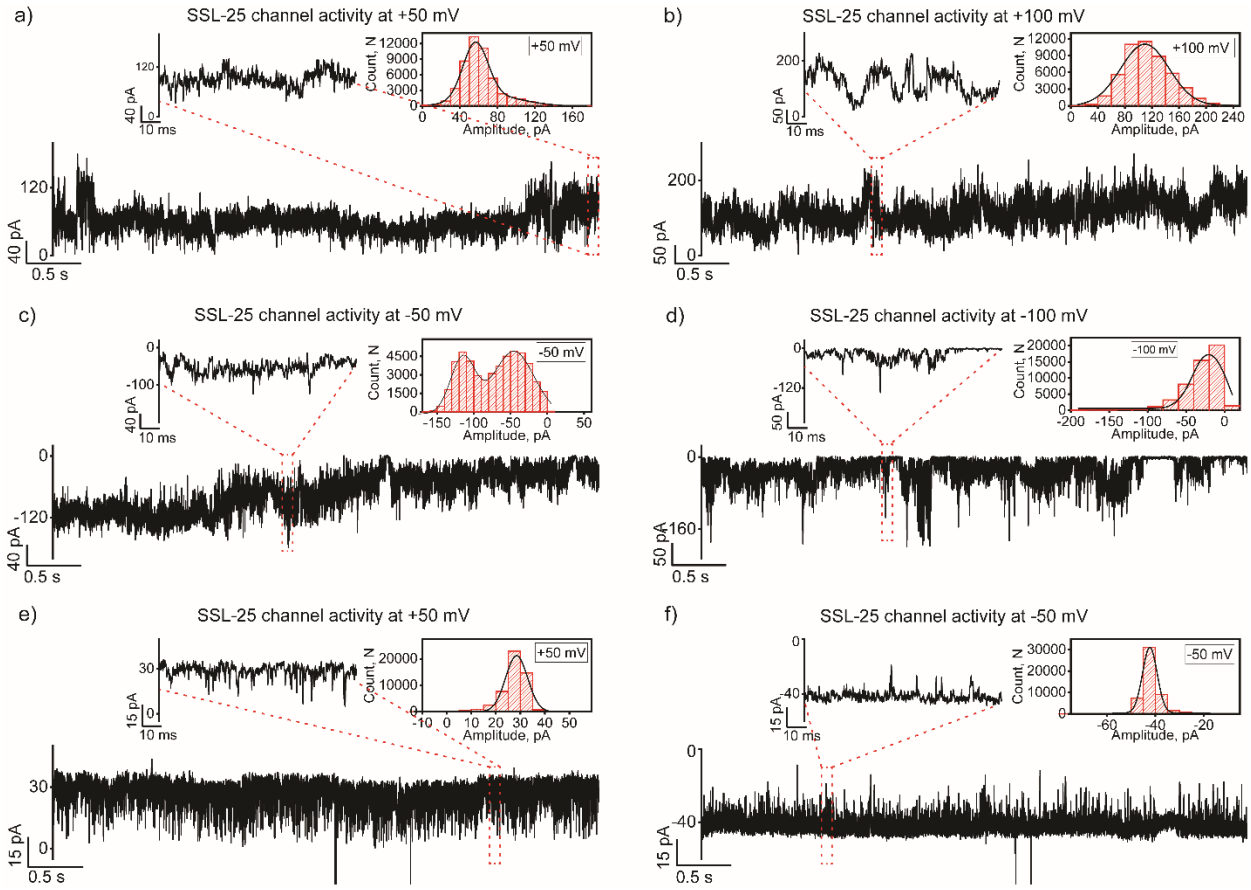

Figure S10: Electrical recordings of SSL-25 dermcidin in planar lipid bilayers

Electrical recording of DCD SSL-25 peptide pores in planar lipid bilayer at **a)** +50 mV and **b)** +100 mV, **c)** -50 mV, **d)** -100 mV showing fluctuating and stable asymmetrical conductance states. The frequency of gating increased with increasing voltage. Electrical recording of DCD-SSL-25 peptide pores showing a stable channel at **e)** +50 mV and **f)** -50 mV, Inset represents corresponding all points current amplitude histogram and ion current recordings at expanded time scale. Reaction conditions: 1M KCl, 10mM MES, pH 6.0

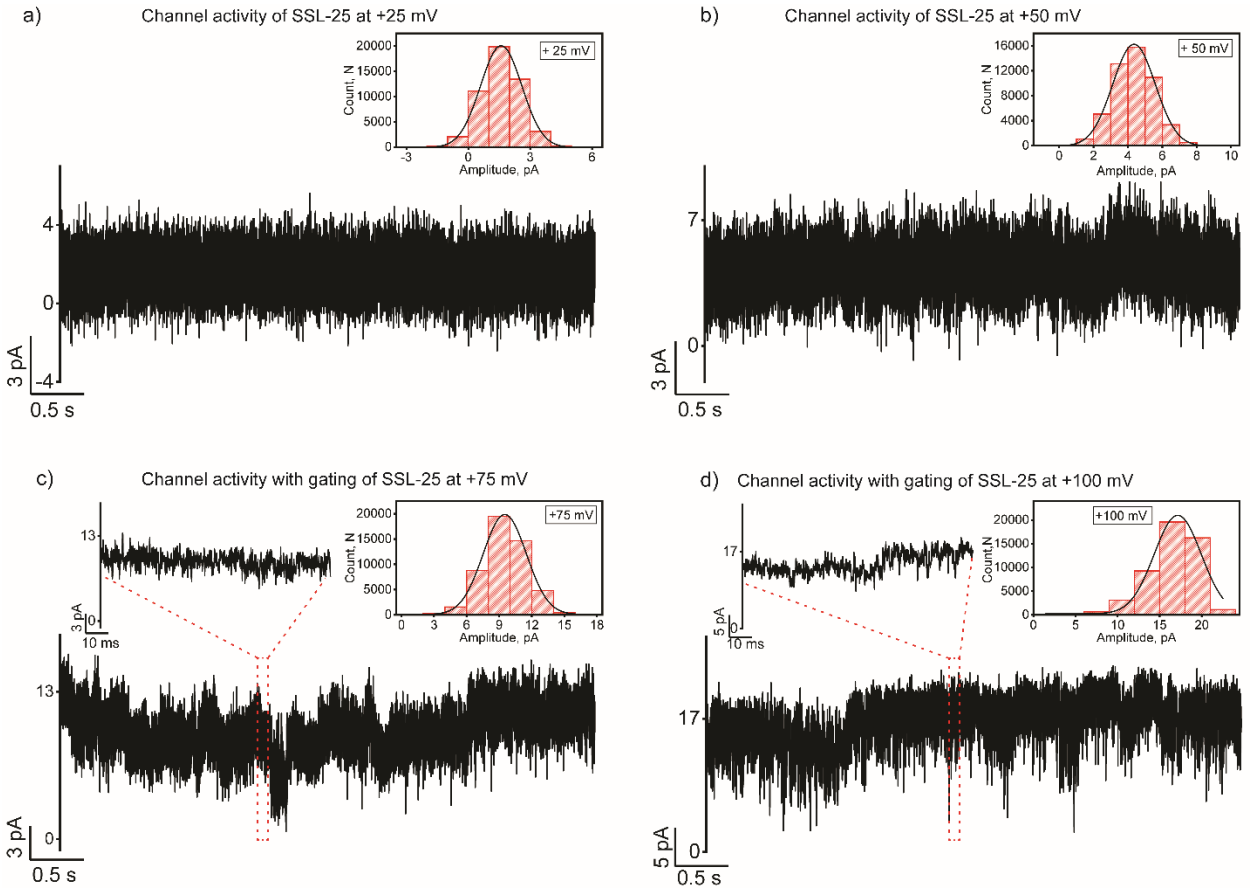

Figure S11: Electrical recordings of DCD SSL-25 showing gating in planar lipid bilayers in asymmetrical conditions

Electrical recording of DCD SSL-25 peptide reconstituted in planar lipid bilayer showing various gating patterns at different voltages a) +25 mV, b) +50 mV, c) +75 mV and d) +100 mV. Inset represents corresponding all points current amplitude histogram and ion current recordings at expanded time scale. Reaction conditions: 1M KCl, 10mM MES, pH 6.0 cis/ 0.15 M KCl, 10 mM MES, pH 6.0 trans.

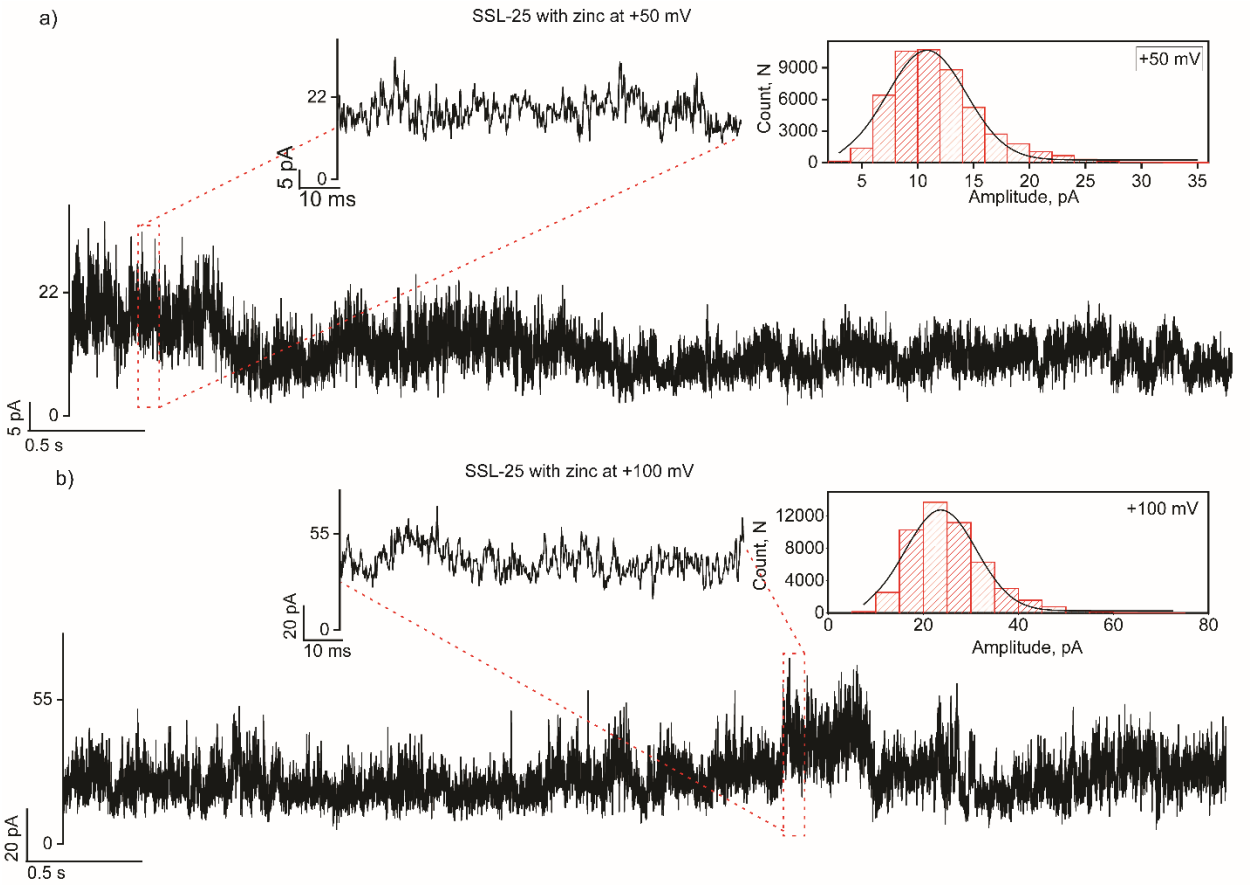

Figure S12: Electrical recordings of dermcidin DCD SSL-25 peptides in planar lipid bilayers in the presence of Zinc ions.

a) Electrical recording of DCD SSL-25 peptide channels in planar lipid bilayers in the presence of 1mM $ZnCl_2$ at +50 mV showing fluctuating and stable conductance states. **b)** Electrical recording of DCD SSL-25 peptide pores in planar lipid bilayers in the presence of 1mM $ZnCl_2$ at +100 mV showing fluctuating and stable conductance states. Inset represents corresponding all points current amplitude histogram and ion current recordings at expanded time scale. Reaction conditions: 1M KCl, 10mM MES, pH 6.0, 1mM $ZnCl_2$.

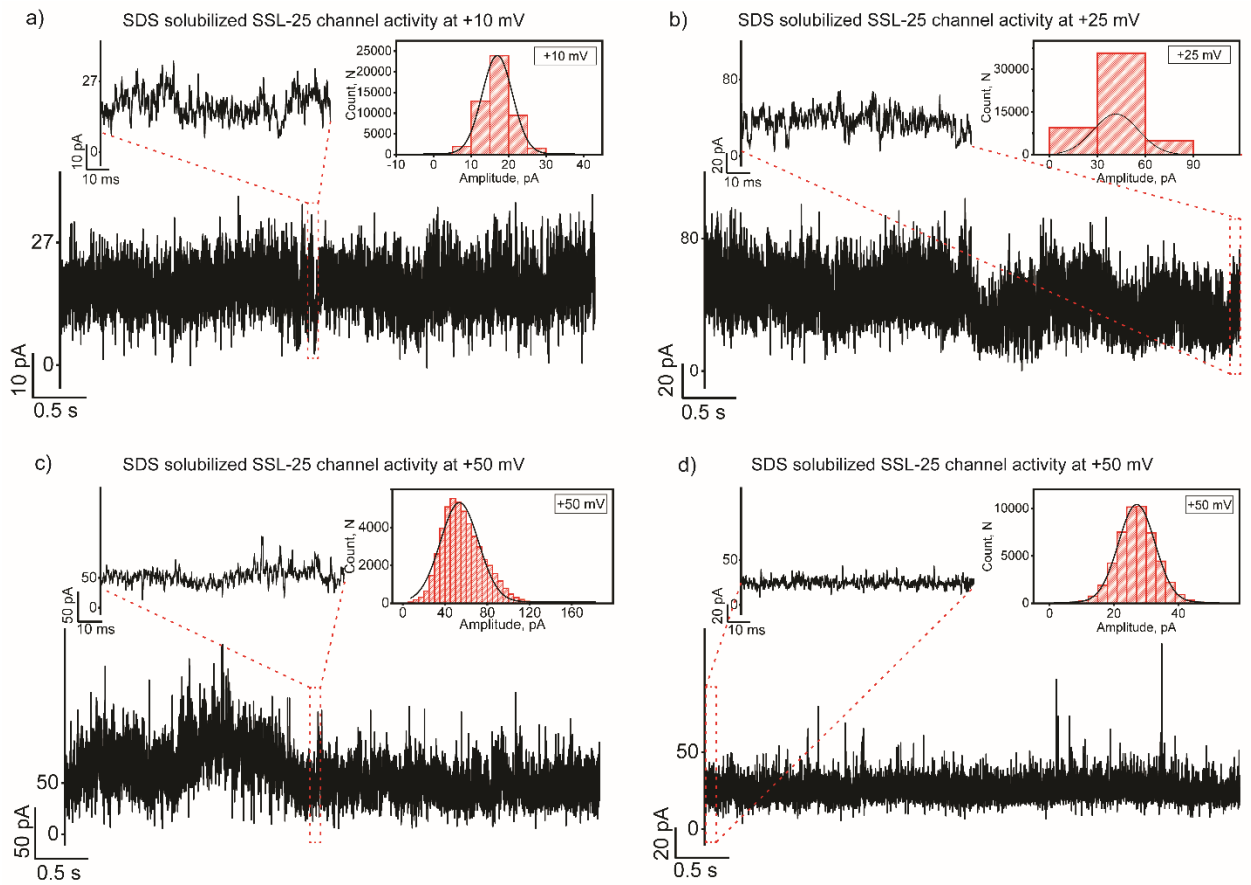

Figure S13: Electrical recordings of SDS-solubilized DCD SSL-25 in planar lipid bilayers

a) Electrical recording of SDS solubilized DCD SSL-25 peptide channel in planar lipid bilayer at +10 mV. **b)** Electrical recording of DCD SSL-25 channel showing channel activity at +25 mV. **c)**, **d)** Electrical recording of DCD SSL-25 channel showing channel activity with increased gating events at +50 mV. Inset represents corresponding all points current amplitude histogram and ion current recordings at expanded time scale. Reaction conditions: 1M KCl, 10mM MES, pH 6.0

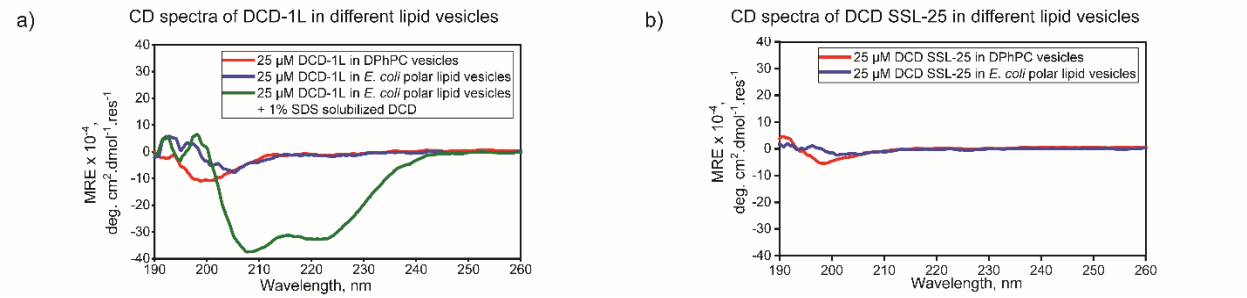

Figure S14: CD spectra of DCD peptides in lipid vesicles

a) CD spectra at 20°C for DCD-1L in PBS with DPhPC lipids at 25 μM (red) and E. coli polar lipid extracts at 25 μM (blue) peptide concentration. Addition of 1% SDS solubilized DCD-1L to lipid vesicles resulted in alpha-helical conformation (green) **b)** CD spectra at 20°C for DCD SSL-25 peptide in PBS with DPhPC lipids at 25 μM (red) and E. coli polar lipid extracts at 25 μM (blue) peptide concentration.

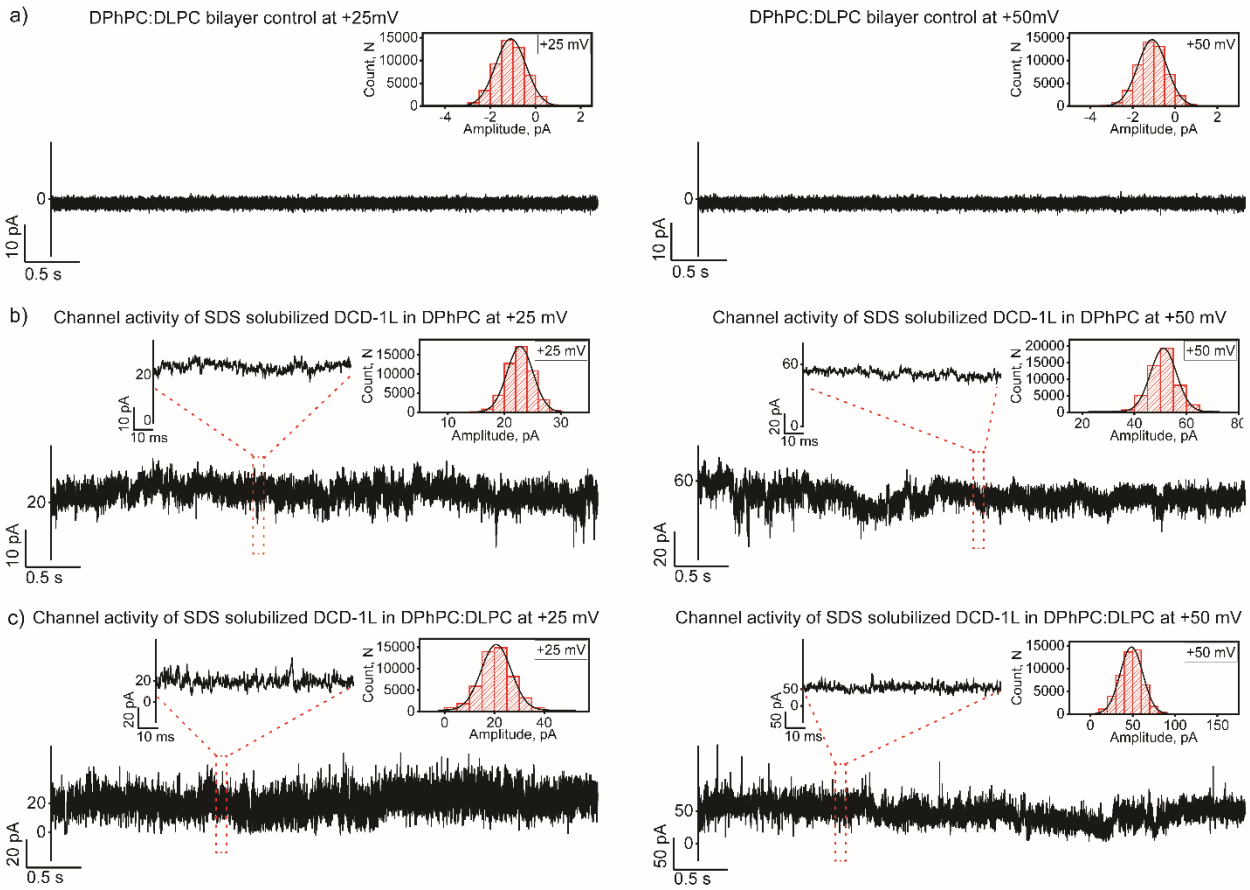

Figure S15: Electrical recordings of DCD-1L channel activity in DPhPC: DLPC bilayers

a) Electrical recording of stable DPhPC: DLPC bilayers at +25 and +50 mV. **b)** Electrical recording of 1% SDS solubilized DCD-1L peptide reconstituted in planar lipid bilayer formed from 100% DPhPC lipids showing stable channel at +25 mV and +50 mV. **c)** Electrical recording of 1% SDS solubilized DCD-1L peptide reconstituted in planar lipid bilayer formed from 90% DPhPC and 10% DLPC lipids showing stable channel at +25 mV and +50 mV. Inset represents corresponding all points current amplitude histogram and ion current recordings at expanded time scale. Reaction conditions: 1M KCl, 10mM MES, pH 6.0, 1mM $ZnCl_2$.

References:

1. C. Song, C. Weichbrodt, E. S. Salnikov, M. Dynowski, B. O. Forsberg, B. Bechinger, C. Steinem, B. L. de Groot, U. Zachariae and K. Zeth, *Proc. Natl. Acad. Sci. USA.*, 2013, **110**, 4586-91.

2. R. Benz, A. Schmid, R.E Hancock, *J. Bacteriol.,* 1985, **162** , 722-7.

3. H. Bajaj, M. A Scorciapino, L. Moynié, M. G Page, J. H Naismith, M. Ceccarelli, M. Winterhalter, *J. Biol. Chem.* 2016, **291**, 2837-47.